The Astrophysical Journal, 634:1126–1132, 2005 December 1

THE $^{12}C/^{13}C$ ISOTOPE GRADIENT DERIVED FROM MILLIMETER TRANSITIONS OF CN: THE CASE FOR GALACTIC CHEMICAL EVOLUTION

S. N. Milam, C. Savage,[1] M. A. Brewster,[2] and L. M. Ziurys
Department of Chemistry, Department of Astronomy, and Steward Observatory, 933 North Cherry Avenue, University of Arizona, Tucson, AZ 85721

and

S. Wyckoff
Department of Physics and Astronomy, Arizona State University, Tempe, AZ 85287
Received 2005 April 8; accepted 2005 August 16

ABSTRACT

New measurements of $^{12}C/^{13}C$ ratios in Galactic molecular clouds have been conducted using the $N = 1 \rightarrow 0$ transition of the CN radical. This species is unique in that it has extensive hyperfine structure that can be accurately used to correct for line saturation effects. Combined with the past observations of Savage and coworkers, the ratios derived from CN are the most extensive data set to date for molecular clouds, and they include sources that lie in the range of 0.09–16.41 kpc in distance from the Galactic center (D_{GC}). The ratios derived from CN indicate a gradient with Galactic distance of $^{12}C/^{13}C = 6.01D_{GC} + 12.28$. This gradient agrees rather closely with those derived from measurements of CO and H_2CO. The least-squares fit to all data points for the three molecules is $^{12}C/^{13}C = 6.21D_{GC} + 18.71$. CO, CN, and H_2CO are synthesized from quite varied reactions, and any ^{13}C fractionation must follow different pathways for these three species. The relatively good agreement between the $^{12}C/^{13}C$ ratios of the three molecules, as well as their lack of correlation with gas kinetic temperature, suggests that chemical fractionation and isotope-selective photodissociation both do not play a substantial role in influencing such ratios. Therefore, the $^{12}C/^{13}C$ gradient found in the Galaxy is a true indicator of Galactic chemical evolution. The apparent discrepancy between the solar system ($^{12}C/^{13}C = 89$) and local interstellar medium values ($^{12}C/^{13}C \approx 68$) of this ratio may be a result of ^{13}C enrichment since the formation of the solar system, as predicted by recent models.

Subject headings: astrochemistry — Galaxy: evolution — ISM: abundances — ISM: clouds — radio lines: ISM — stars: AGB and post-AGB

1. INTRODUCTION

Observations of isotopic abundances in the interstellar medium provide an avenue for a quantitative assessment of stellar nucleosynthesis and therefore Galactic chemical evolution (GCE). For example, the $^6Li/^7Li$ ratio places constraints on the formation of lithium after the big bang, as well as providing insight into the destruction mechanisms of these isotopes (Aoki et al. 2004). The $^{12}C/^{13}C$ isotope ratio is also considered an important tracer, because it reflects the relative degree of primary to secondary processing in stars. ^{12}C is predicted to be formed in the triple alpha reaction (Timmes et al. 1995); in massive stars, extremely high temperatures due to gravitational collapse initiate the formation of carbon through the fusion of three alpha particles. ^{13}C is a reaction intermediate in the carbon-nitrogen-oxygen (CNO) cycle, which occurs in asymptotic giant branch (AGB) stars (Pagel 1997). These objects have a carbon/oxygen core surrounded by helium- and hydrogen-burning shells. As nuclear burning takes place in each shell, they eventually become unstable due to the loss of fuel, leading to gravitational collapse followed by rapid expansion, otherwise known as "helium flashes." Once the helium shell becomes convectively unstable, processed material from the core of the star is pulled to the surface; this convective mixing is known as the "third dredge-up" (e.g., Herwig & Austin 2004). In the course of this dredge-up, the intermediate product, ^{13}C, is mixed into the expanding atmosphere of the star, where it is then ejected into the interstellar medium (ISM). The dredge-up properties of AGB stars are not well understood (Herwig & Austin 2004), but obviously have a significant impact on interstellar isotope abundances.

Numerous studies of the $^{12}C/^{13}C$ ratio have been conducted toward molecular clouds throughout the Galaxy (e.g., Wilson & Rood 1994; Penzias 1980; Langer & Penzias 1990; Henkel et al. 1983; Gardner & Whiteoak 1979). One of the most common methods of measuring the ratio is to compare line intensities of the ^{12}C and ^{13}C isotopomers of common molecules such as CO, H_2CO, and HCO^+. However, favorable transitions of very abundant molecules are often saturated, and therefore relative line intensities are not necessarily an accurate indicator of isotope ratios (e.g., Langer & Penzias 1990). In the past, this problem has been dealt with by using molecular line modeling or the double isotope ratios. Possible effects of chemical fractionation may also be influencing $^{12}C/^{13}C$ isotope ratios. For example, some molecules such as CO are thought to be preferentially enriched in ^{13}C, because the bond in ^{13}CO is slightly stronger than that in ^{12}CO. Despite these difficulties, molecular line measurements taken over a period of several decades indicate that the $^{12}C/^{13}C$ ratio steadily increases with distance from the Galactic center (e.g., Wilson & Rood 1994). These studies have also suggested that values established from CO serve as a lower limit to the "true" $^{12}C/^{13}C$ isotope ratio gradient, while those from H_2CO reflect the upper range (Wilson & Rood 1994).

In order to further examine $^{12}C/^{13}C$ ratios, we have conducted new observations of ^{12}CN and ^{13}CN toward Galactic molecular

[1] Current address: JILA, NIST, and University of Colorado, Boulder, CO 80309.
[2] Current address: Sfyri, Inc., P. O. Box 19742, Seattle, WA 98109.

TABLE 1

COMPARISON OF $^{12}C/^{13}C$ RATIOS OBSERVED IN MOLECULAR CLOUDS FROM CN, CO, AND H_2CO

SOURCE	l (deg)	b (deg)	D_{GC} (kpc)	D_z (kpc)	T_k (K)	τ_{total}[a]	T_{ex}[a] (K)	$^{12}C/^{13}C$ CN[b]	$^{12}C/^{13}C$ CO[c]	$^{12}C/^{13}C$ H_2CO[d]	$^{12}C/^{13}C$ Average
Sgr B2(OH)	0.662	−0.041	0.1	−0.01	30	...	...	$\geq 18_{-6}$[e]	24 ± 1	10	17
G29.9	29.930	−0.050	4.1	−0.01	20	2.55 ± 0.92	5.10 ± 0.72	63 ± 27	...	45 ± 5	54
G49.2	49.204	−0.345	6.3	−0.04	20	...	...	$\geq 33_{-13}$[f]	...	58 ± 4	46
W33	12.799	−0.209	4.1	−0.02	25	...	...	37 ± 8[e]	39 ± 1, 43 ± 4[g]	100	55
G19.6	19.608	−0.235	4.3	−0.02	20	4.24 ± 0.89	3.39 ± 0.08	71 ± 17	...	41 ± 4	56
W31	10.150	−0.340	3.1	−0.03	18	1.42 ± 0.34	6.95 ± 0.85	20 ± 6	...	37 ± 6	29
G34.3	34.258	0.153	5.1	0.01	25	...	...	28 ± 4[e]	...	58 ± 5	43
G35.2	35.194	−1.750	5.7	−0.09	20	2.78 ± 1.00	4.49 ± 0.40	64 ± 24	...	55 ± 5	60
W51M	49.490	−0.387	6.1	−0.04	30	...	...	35 ± 12[e]	45 ± 2	...	40
W49	43.170	0.011	7.8	0.01	35	...	...	44 ± 22[e]	49 ± 6	74 ± 20	56
DR 21(OH)	81.720	0.570	8.	0.03	25	...	...	36 ± 3[e]	53 ± 2	66	52
Orion A	208.992	−19.385	8.3	−0.16	80	...	...	43 ± 7[e]	79 ± 7	...	61
NGC 2024	206.557	−16.361	8.3	−0.12	40	...	...	65 ± 12[e]	...	68 ± 11	67
Orion Bar	209.050	−19.382	8.3	−0.16	50	...	...	70 ± 11[e]	75 ± 9[h]	...	73
NGC 7538	111.542	0.776	8.9	0.03	24	...	...	56 ± 10[e]	...	...	56
W3(OH)	133.950	1.064	9.6	0.04	20	...	...	63 ± 16[e]	66 ± 4, 85 ± 15[g]	91 ± 16	76
S156	110.110	0.050	10.9	0.01	20	1.03 ± 0.49	6.57 ± 1.59	78 ± 44	...	...	78
WB89 391	125.807	3.050	16.4	0.56	16	3.20 ± 0.75	2.90 ± 0.03	134 ± 43	...	...	134

[a] Total optical depth (τ_{total}) and excitation temperatures (T_{ex}) derived from CN (see text).
[b] Derived from the $N = 1 \rightarrow 0$ transition.
[c] Derived from the $J = 1 \rightarrow 0$ transition by Langer & Penzias (1990) except where indicated.
[d] Derived from the $J_{K_a,K_c} = 1_{10} \rightarrow 1_{11}$ and the $J_{K_a,K_c} = 2_{11} \rightarrow 2_{12}$ transitions by Henkel et al. (1980, 1982, 1983, 1985).
[e] From Savage et al. (2002).
[f] Calculated in the thin limit.
[g] From Wouterloot & Brand (1996).
[h] From Keene et al. (1998).

clouds. This work is an extension of a study previously carried out by Savage et al. (2002). CN is a unique tracer of this ratio, because the hyperfine structure present within a given rotational transition enables an accurate assessment of the line opacity (Savage et al. 2002). Thus, more accurate values of the $^{12}C/^{13}C$ isotope ratio can be determined. In this paper we present the latest results of millimeter observations of the $N = 1 \rightarrow 0$ transitions of ^{12}CN and ^{13}CN, which include measurements at the far edges of the Galaxy. In conjunction with the past data of Savage et al. (2002), the ratio has been measured over the entire range of 0.1–16.4 kpc from the Galactic center. Here we present out results, compare them with ratios derived from other molecules, and discuss the implications for GCE.

2. OBSERVATIONS

Measurements of the $N = 1 \rightarrow 0$ rotational transitions of ^{12}CN and ^{13}CN were carried out during the period 2002 September–2004 June. The observations were made using the Kitt Peak 12 m telescope of the Arizona Radio Observatory (ARO).[3] The receivers used were dual-channel SIS mixers operated in single-sideband mode with image rejection around 20 dB. The back ends employed were filter banks with 100 kHz, 250 kHz, 500 kHz, or 1 MHz resolutions, depending on the source. The observing frequencies used were 113490.98 MHz for ^{12}CN and 108780.2 MHz for ^{13}CN; the telescope beam size was 58″–59″ at these frequencies. The temperature scale is given in terms of T_R^*, which is the chopper-wheel antenna temperature corrected for forward spillover losses (η_{fss}). The radiation temperature is then determined using η_c, the corrected beam efficiency, where $T_R = T_R^*/\eta_c$. All data were taken in position-switching mode with an off position 30′ west in azimuth. To ensure positional accuracy, periodic pointing and focusing on planets was conducted.

[3] The Kitt Peak 12 m telescope is currently operated by the Arizona Radio Observatory, at Steward Observatory (University of Arizona), with partial support from the Research Corporation.

3. RESULTS AND ANALYSIS

3.1. $^{12}C/^{13}C$ *Isotope Ratios from* CN

The observations of the $N = 1 \rightarrow 0$ transitions of ^{12}CN and ^{13}CN were made toward seven molecular clouds across the Galaxy. Such clouds generally have low kinetic temperatures. In these objects, emission is thought to arise from the cold extended material. The new sources and those of Savage et al. (2002) are listed in Table 1, along with their Galactic (l, b) coordinates, kinetic temperatures, and distances to the Galactic center D_{GC} (assuming a solar distance of 7.9 kpc; McNamara et al. 2000). These clouds were chosen based on their strategic locations throughout the Galaxy. These new data expand the original set of Savage et al. (2002) by including sources between 0 and 6 kpc and beyond 10 kpc. A total of 18 self-consistent data points are consequently available for examining a Galactic gradient from CN—more than previous sets of CO and H_2CO data (see Wilson & Rood 1994). The details of these measurements will be given in a later paper (S. N. Milam et al. 2005, in preparation).

An example of the observational data is shown in Figure 1, which presents spectra observed toward the molecular cloud S156. The $N = 1 \rightarrow 0$ rotational transitions of both ^{12}CN (*top:* $J = 3/2 \rightarrow 1/2$ spin component) and ^{13}CN (*bottom:* $F_1 = 1 \rightarrow 0, F_2 = 2 \rightarrow 1$ spin component) are displayed. Each transition is further split into hyperfine components, whose relative intensities are plotted beneath the observed spectra. As shown in Figure 1, this transition of ^{12}CN consists of five individual hyperfine

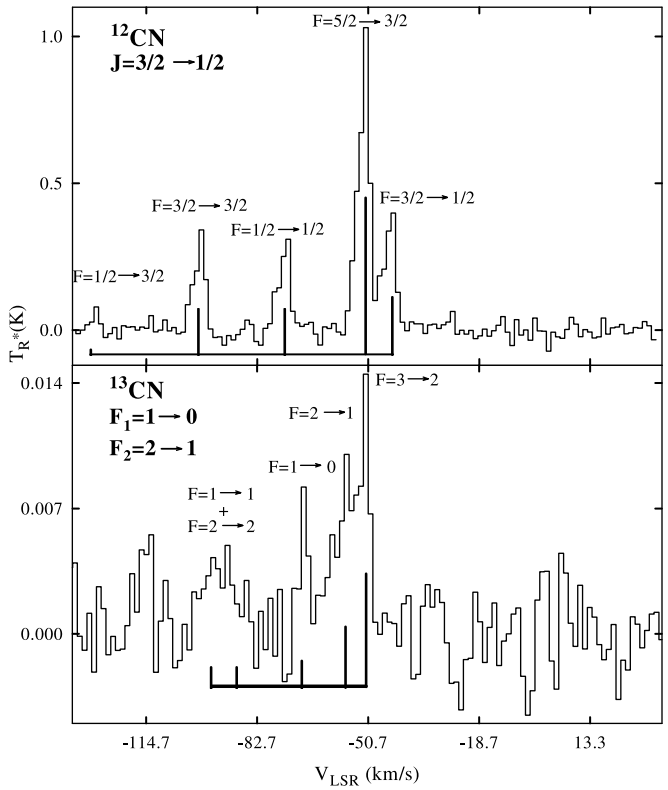

FIG. 1.—Representative spectra of the $N = 1 \rightarrow 0$ transition of ^{12}CN (*top:* $J = 3/2 \rightarrow 1/2$ spin component) at 113 GHz and ^{13}CN (*bottom:* $F_1 = 1 \rightarrow 0$, $F_2 = 2 \rightarrow 1$ spin component) at 109 GHz observed toward the molecular cloud S156 using the ARO 12 m telescope. The spectra were recorded with 500 kHz resolution (1.32 km s^{-1}). The positions and intensities of the hyperfine components, indicated by quantum number F, are shown under the spectra. The hyperfine structure in CN is a direct measure of the opacity in these lines.

(hf) components, indicated by the quantum number F, which were all resolved in the spectrum. The hf structure arises from the nuclear spin of nitrogen ($I = 1$). The same transition in ^{13}CN also consists of five hyperfine components, but these lie closer in frequency, and hence some are blended together. They also have considerably weaker brightness temperatures. Furthermore, the ^{13}CN spectrum is more complicated, because the ^{13}C nucleus has a spin of $I = 1/2$. Hence, two spins are coupled to the rotational motion to generate quantum numbers F_1, F_2, and F. The lines shown here correspond to $N = 1 \rightarrow 0$, $F_1 = 1 \rightarrow 0$, and $F_2 = 2 \rightarrow 1$.

The ^{12}C/^{13}C isotope ratio is directly evaluated by comparing the line intensities of the $N = 1 \rightarrow 0$ transitions of ^{12}CN to those of ^{13}CN, corrected for the relative intensities of the hf components, provided the lines are optically thin. The line intensities and their uncertainties were determined by Gaussian fits to the spectral profiles. Low opacities are indicated by line intensities that match the theoretical predictions, of which the spectra from S156 are an example. Some of the ^{12}CN transitions, however, are saturated, as indicated by the less-favored hyperfine lines, which exhibit higher intensities than predicted relative to the main hf feature. To correct for these saturation effects, the relative intensities of the hyperfine components can be compared to determine τ, the optical depth, for that particular source by using the relationship (Savage et al. 2002)

$$\frac{T_R^*(\mathrm{hf})}{T_R^*(\mathrm{hf_{main}})} = \frac{1 - e^{-R_{\mathrm{hf}}\tau}}{1 - e^{-\tau}}. \quad (1)$$

Here T_R^* is the observed line intensity for a particular hf component and R_{hf} is its theoretical relative intensity. When a given transition is saturated, the line intensity is not an accurate measurement of the amount of ^{12}CN. In this case, the opacity and excitation temperature are used instead to determine the quantity of ^{12}CN (see Savage et al. 2002 for a complete discussion).

One molecular cloud (G49.2) showed evidence of self-absorption in its ^{12}CN spectrum. In this case, the intensity of the weakest hf component ($F = 1/2 \rightarrow 3/2$, 1.23%) of ^{12}CN had to be used to estimate the ratio in the thin limit. However, even this component could be slightly self-reversed; therefore, only a lower limit to the true ratio could be determined.

Table 1 lists the opacity τ, excitation temperature T_{ex} (K), distance to the Galactic center D_{GC} (kpc), distance above/below the Galactic plane D_z (kpc), and ^{12}C/^{13}C isotope ratios derived from CN, CO, and H_2CO. The ^{12}C/^{13}C isotope ratios from CN include those from Savage et al. (2002). The average ^{12}C/^{13}C ratios were also derived from the three molecules toward a given source.

3.2. *The Galactic* ^{12}C/^{13}C *Gradient*

The complete set of ^{12}C/^{13}C ratios established from CN was plotted as a function of distance from the Galactic center D_{GC} and is shown in Figure 2. The gray squares are the new values presented in this paper, while the black diamonds are those from Savage et al. (2002). Errors are 1 σ. A linear fit to the combined CN data is indicated by the solid black line. (G49.2 was not included in this fit, because the ratio is only a lower limit.) The y-intercept is ^{12}C/^{13}C ~ 12. A positive Galactic gradient is apparent in the isotope ratios.

Also shown in Figure 2 are the gradients determined for CO and H_2CO. The CO isotope data (*gray dashed line*) are from Langer & Penzias (1990, 1993), Keene et al. (1998), and Wouterloot & Brand (1996), while the H_2CO values (*black dash-dotted line*) are from Henkel et al. (1980, 1982, 1983, 1985), Gardner & Whiteoak (1979), and Güsten et al. (1985). These molecular species show a positive Galactic gradient as well. Unweighted least-squares fits to these individual data sets yield

$$\mathrm{CN}, \quad {}^{12}\mathrm{C}/{}^{13}\mathrm{C} = 6.01(1.19)D_{\mathrm{GC}} + 12.28(9.33), \quad (2)$$

$$\mathrm{CO}, \quad {}^{12}\mathrm{C}/{}^{13}\mathrm{C} = 5.41(1.07)D_{\mathrm{GC}} + 19.03(7.90), \quad (3)$$

$$\mathrm{H_2CO}, \quad {}^{12}\mathrm{C}/{}^{13}\mathrm{C} = 7.60(1.79)D_{\mathrm{GC}} + 18.05(10.88). \quad (4)$$

The least-squares fit to all data points for these three molecules using all available data from the literature, shown by the gray dotted line, is

$$^{12}\mathrm{C}/{}^{13}\mathrm{C} = 6.21(1.00)D_{\mathrm{GC}} + 18.71(7.37). \quad (5)$$

The CO fit was determined primarily from surveys conducted by Langer & Penzias (1990, 1993), but other data points were included. Wouterloot & Brand (1996), however, have determined a lower limit to the ^{12}C/^{13}C ratio from CO in the outer Galaxy at 13.7 kpc toward WB89 437. If this limit of $^{12}\mathrm{C}/{}^{13}\mathrm{C} \geq 201 \pm 15$ is included in the CO data, the resulting fit yields

$$\mathrm{CO}, \quad {}^{12}\mathrm{C}/{}^{13}\mathrm{C} = 10.63(2.32)D_{\mathrm{GC}} - 12.01(18.58). \quad (6)$$

This fit varies quite significantly from the previous ones, and the value of the y-intercept is negative and hence not physical.

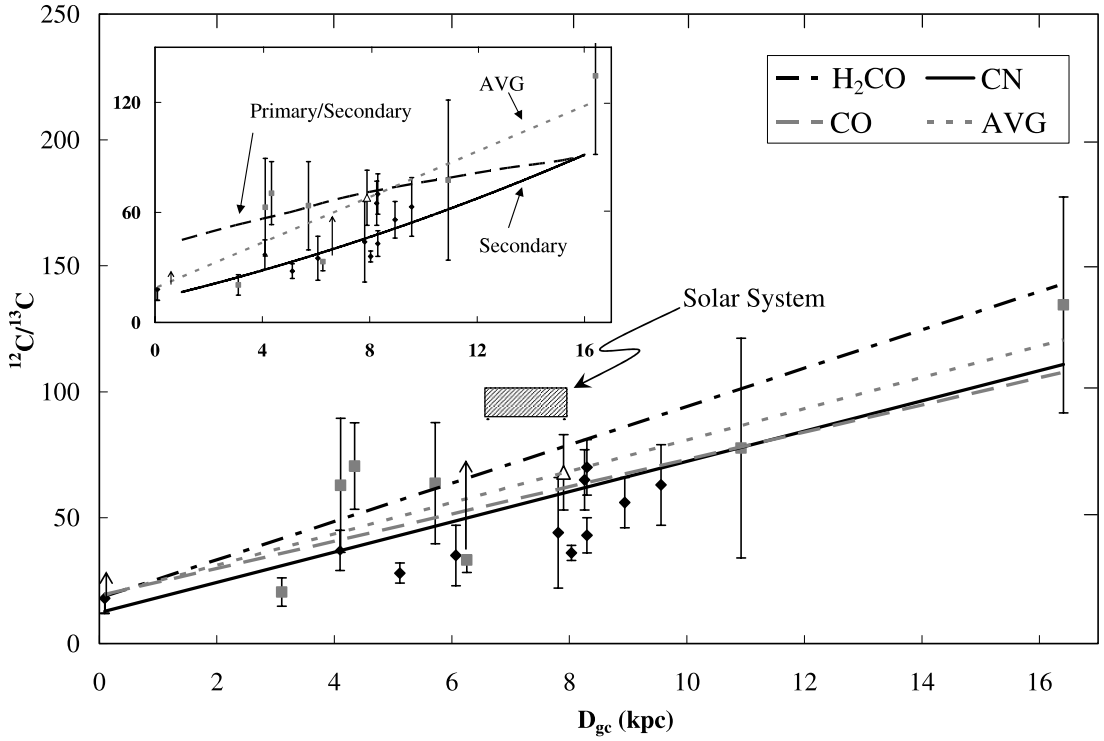

FIG. 2.—Plot of $^{12}C/^{13}C$ isotope ratios as a function of distance to the Galactic center, D_{GC} (kpc). The solar distance to the Galactic center is assumed to be 7.9 kpc. The gray squares are values of $^{12}C/^{13}C$ ratios derived in the current work, and the black diamonds are values from Savage et al. (2002), both from CN $N = 1 \rightarrow 0$ measurements conducted at the ARO 12 m telescope. A linear fit of the ratios derived from CN is plotted as a solid black line. The isotope gradient derived from CO is indicated by the gray dashed line, and the black dash-dotted line represents that resulting from H_2CO data. The gray dotted line represents the least-squares fit to all data points from the three molecules. The hatched box represents the range of $^{12}C/^{13}C$ isotope ratios for the solar system (89 meteorite organics, 100 solar wind lunar regoliths, 6.6 kpc initial Sun orbit, and 7.9 kpc current Sun galactocentric distance). The open triangle represents the average local ISM carbon isotope ratio of 68 ± 15 (this study; S. N. Milam et al. 2005, in preparation). The inset shows the $^{12}C/^{13}C$ isotope ratios from CN as a function of D_{GC} along with the model by Prantzos et al. (1996). The dashed black line represents the calculation of the ratio assuming that ^{13}C has a mixed primary and secondary source, while the solid line displays the calculations with a purely secondary ^{13}C source. The gray dotted line continues to represent the average for all three molecules: CO, CN, and H_2CO (see text).

Therefore, this data point was not included in the analysis. Obviously, additional ratios are needed for sources with $D_{GC} > 12$ kpc.

4. DISCUSSION

4.1. *A Comparison of* $^{12}C/^{13}C$ *Gradients from* CO, H_2CO, *and* CN

As shown in Figure 2, the $^{12}C/^{13}C$ isotope ratios determined from CN are in reasonable agreement with those of CO and H_2CO. CO and CN display a lower limit of the $^{12}C/^{13}C$ isotope ratio, and H_2CO seemingly provides an upper limit. However, the average fit from all three species does not significantly deviate from the individual fits. For example, within the quoted errors, the slopes and y-intercepts from the three fits agree with each other. All fits also provide a Galactic center value of $^{12}C/^{13}C \sim 20$. It should additionally be noted that only the CN data set provides ratios beyond 10 kpc.

4.2. *Effects of Isotope-selective Photodissociation*

Isotope-selective photodissociation, which occurs when a large UV flux is present near a molecular cloud (Savage et al. 2002), can potentially influence the $^{12}C/^{13}C$ ratio. Molecules containing ^{12}C are more abundant than those with ^{13}C and hence are self-shielding to photodissociation, unlike their ^{13}C counterparts. The $^{12}C/^{13}C$ ratio should therefore increase in regions of high UV radiation. Most giant molecular clouds are near H II regions and thus are subject to such fields. In photon-dominated regions (PDRs) this effect is particularly pronounced, and these sources should consequently exhibit higher $^{12}C/^{13}C$ ratios. Two such PDRs, the Orion Bar and NGC 2024, have been included in this survey. They do not appear, however, to exhibit particularly high ratios relative to other sources.

The $N = 1 \rightarrow 0$ transition of CN, in addition, has a critical density on the order of $\sim 2 \times 10^5$ cm^{-3} for collisional excitation, whereas the $J = 1 \rightarrow 0$ transition of CO requires a density of merely ~ 1000 cm^{-3}. The CN emission observed must arise from dense gas, where UV flux can only partially penetrate. In contrast, CO is present in the more diffuse material; it is also 10,000 times more abundant than CN. Consequently, the ratios derived from CO should show a marked increase relative to those established from CN. However, the ratios found from these two molecules in this study are in good agreement, even toward the PDR sources. The isotope-selective photodissociation therefore cannot be significantly influencing the $^{12}C/^{13}C$ ratios.

4.3. *Fractionation in Carbon Isotope Ratios?*

In order to examine the relative chemistries of CN, CO, and H_2CO, a qualitative chemical network has been created for these species and is shown in Figure 3. This network has been compiled from the reactions of Prasad & Huntress (1980a, 1980b) and has been updated using the UMIST database (Le Teuff et al. 2000). The diagram illustrates that each molecular species used in determining carbon isotope ratios has a different major formation pathway. Formaldehyde is created by the neutral-neutral reaction of CH_3 and atomic oxygen; CN is also formed in a neutral-neutral reaction with CH and atomic nitrogen; and multiple reactions, both ion-molecule and neutral-neutral processes, lead to CO. There is no favorable route from CO to CN.

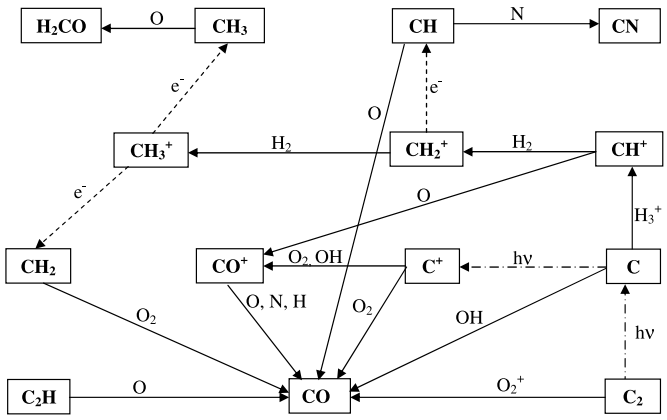

FIG. 3.—Formation pathways leading to CN, H_2CO, and CO in molecular clouds. As the figure illustrates, the reaction networks leading to the three molecules are quite different, suggesting that the ^{13}C enrichment from fractionation should vary considerably between the three species.

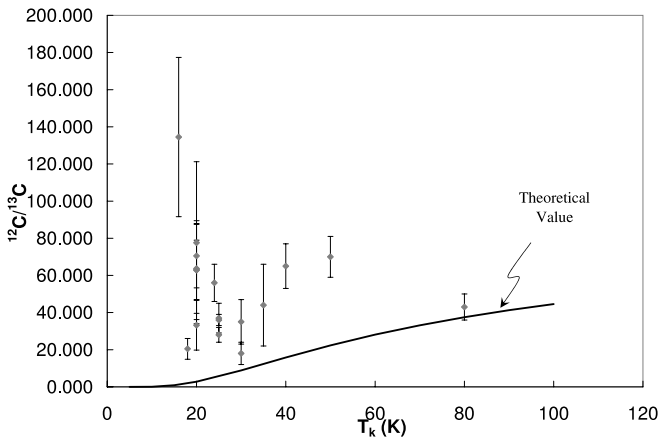

FIG. 4.—Graph of the $^{12}C/^{13}C$ isotope ratios derived from CN plotted against gas kinetic temperature of the respective sources, shown by gray squares. The black curve is the theoretical prediction of ^{13}C enrichment arising from fractionation at equilibrium, from a $^{12}C/^{13}C$ reservoir of 89. There is little correlation between the actual and predicted value.

Chemical fractionation is postulated to affect values of the $^{12}C/^{13}C$ isotope ratios. For simple carbon-containing molecules, fractionation is predicted to occur through the isotopic exchange reactions (Penzias 1980; Langer 1992)

$$^{13}C^+ + {}^{12}CO \xrightarrow{k_1} {}^{13}CO + {}^{12}C^+ + \Delta E, \quad (7)$$

$$^{13}C^+ + {}^{12}CN \xrightarrow{k_2} {}^{13}CN + {}^{12}C^+ + \Delta E. \quad (8)$$

Here ΔE is the zero-point energy difference between the ^{12}C and ^{13}C isotopomers. The reaction involving CO has been studied at 300 K, where the rate has been established to be $k_1 = 2 \times 10^{-10}$ cm^3 s^{-1} and $\Delta E = 35$ K (Watson et al. 1976). The second process has not been studied experimentally, but ΔE has been determined to be 34 K based on the vibrational energy level ($v = 0$) differences (see Langer 1992). Hence, at low temperatures the 34–35 K differences in zero-point energies should favor ^{13}CO and ^{13}CN over their ^{12}C isotopomers, provided the rates of the exchange reactions given above are fast at such temperatures. For formaldehyde, this simplistic treatment does not apply, because the carbon in this molecule is bonded to three other atoms. Thus, ^{12}C cannot be simply exchanged via a reaction with $^{13}C^+$. ^{13}C enrichment in H_2CO must occur via an earlier precursor, perhaps CH^+(see Fig. 3). It should also be noted that one direct route to CO is via C^+. In contrast, C^+ does not appear to be a significant precursor to CN. All three molecules should therefore trace $^{12}C/^{13}C$ ratios that are not correlated with each other.

Given the variations in the respective reaction pathways leading to CO, CN, and H_2CO and the differences in mechanisms of ^{13}C enrichment, the effects of fractionation should vary significantly between the three molecules. Langer et al. (1984) in fact predict that due to chemical fractionation, the $^{12}C/^{13}C$ ratio derived from CO should be anticorrelated with those obtained from other molecules. This effect results from the fact that CO has a very high abundance relative to the other species, such that it becomes a "sink" of ^{13}C. The ratio derived from CO is predicted to be the lowest as a consequence. Looking at the gradients plotted in Figure 2, the ratio derived from CO may reflect a lower limit at large Galactic distances. However, the gradients established independently from CO, CN, and H_2CO are remarkably similar, even though their formation pathways are independent. The gradient from H_2CO lies only slightly above those of CO and CN, even though its formation pathway does not involve C^+. The similarity of all three gradients suggests that chemical fractionation cannot be a dominant effect. Otherwise, the gradients should agree less favorably.

To examine the extent of chemical fractionation, a simple time-dependent model has been constructed involving C, C^+, CN, and CO and two reactions, equations (7) and (8). Initial relative abundances of the reactants used in the model are $C:C^+:CO:CN = 18:8:74:0.0074$ based on Kramer et al. (2004) and our CN data. The initial isotopic composition was assumed to be $^{12}C/^{13}C = 89$. For reactions (7) and (8), a rate of 2×10^{-10} cm^3 s^{-1} was used, as measured for CO (Watson et al. 1976), and reverse rates were estimated from the Gibb's free energy of formation of the respective species. Fractionation of CO and CN was assumed to occur only through C^+. The calculations were carried out for a typical lifetime of a molecular cloud, 10^6 yr.

These calculations show that for timescales of molecular clouds, chemical fractionation by the C^+ mechanism is negligible, given a temperature range of $T_k = 10-100$ K. For example, the $^{12}C/^{13}C$ ratio at 10^5 yr for a cloud at 50 K, derived from both CO and CN, is 89. In fact, the isotope ratio did not vary significantly from 89 over the whole temperature range for both CO and CN. At 10^6 yr, only a 1.7% decrease in the $^{12}CO/^{13}CO$ ratio at 30 K and lower was found in both molecules.

Further evidence that fractionation is negligible is illustrated in Figure 4. Here the $^{12}C/^{13}C$ ratios derived from CN are plotted against gas kinetic temperature, T_k, for the molecular clouds studied, denoted by gray squares. Kinetic temperatures (Table 1) were obtained from Mangum et al. (1991, 1999), van der Werf et al. (1996), Carral & Welch (1992), White et al. (1982), Jaffe et al. (1989), Apponi et al. (1999), Churchwell et al. (1992), Lis & Goldsmith (1991), Wouterloot & Brand (1996), Langer & Penzias (1990), Henkel et al. (1980, 1985), Dickel et al. (1981), Goldsmith & Mao (1983), and Blitz et al. (1982). There is no obvious correlation between the ratio and T_k. In fact, a wide range of ratios is found around $T_k \sim 20-30$ K. For comparison, the expected $^{12}C/^{13}C$ ratio at chemical equilibrium for CN is also plotted versus kinetic temperature, assuming a zero-point energy difference of 34 K and a $^{12}C/^{13}C$ reservoir of 89. This ratio is shown by the black curve, which predicts significant enrichment in ^{13}C at $T_k \leq 60$ K. There is little correlation between the curve and the observed ratios. Although chemistry in the interstellar

medium is not necessarily at equilibrium, the contrast between the predicted and observed values is striking.

4.4. *Implications for Galactic Chemical Evolution*

Changes in the ISM carbon isotope abundance ratios occur over Galactic timescales as a function of (1) galactocentric distance and (2) time. The distance–$^{12}C/^{13}C$ abundance correlation evident in Figure 2 confirms previous studies (Langer & Penzias 1990, 1993; Wilson & Rood 1994; Savage et al. 2002) and matches expectations of simple theories of nucleosynthesis and GCE (e.g., Prantzos & Aubert 1995; Prantzos et al. 1996; Pagel 1997).

The primary source of interstellar ^{12}C is thought to be massive stars ($M > 6\ M_\odot$) that evolve through core collapse to become Type II supernovae (SNe II). Additional, steadily increasing contributions of ^{12}C to the ISM are postulated to arise from (1) C/O white dwarfs that accrete material from binary companions and evolve into Type Ia supernovae (SNe Ia), and (2) AGB stars that eject nucleosynthesis products in stellar winds and planetary nebulae. Roughly half the observed ^{12}C is thought to have been expelled from SNe II, and half ejected by AGB stars (e.g., Iben & Renzini 1983, 1984; Boothroyd & Sackmann 1999; Clayton 2003). Stellar evolutionary timescales are steep functions of initial masses. Stars with masses $M > 6\ M_\odot$ become SNe II on rapid timescales ($<10^8$ yr) and contribute freshly synthesized elements to the ISM at early Galactic epochs, while ^{12}C contributions from smaller mass (1.5–6 $M_\odot$) AGB stars and SNe Ia are delayed due to the longer stellar evolutionary timescales ($>10^8$ yr). Low- to intermediate-mass stars ($M < 6\ M_\odot$) evolve to the AGB third dredge-up stage or become SNe Ia on timescales $>10^8$ yr (e.g., Clayton 1983). Low-mass stars ($M < 1.5\ M_\odot$) have barely had sufficient time to evolve to the AGB stage (timescale $\sim 10^{10}$ yr) and so contribute negligibly to the ISM enrichment.

Nearly all of the observed ^{13}C is thought to be produced directly from ^{12}C in the CN cycle and is ejected from intermediate-mass (1.5–6 $M_\odot$) AGB stars (Iben & Renzini 1983; Clayton 2003). The onset of the ^{13}C contribution to the ISM is speculated to be delayed from the initial Galactic epochs, because this isotope is probably produced predominantly in low- to intermediate-mass AGB stars, which have long evolutionary timescales relative to the age of the Galaxy. Since star formation tracks the regions of highest gas density, the increase of the $^{12}C/^{13}C$ ratio with galactocentric distance can be understood as gradual depletion of ^{12}C and enrichment of ^{13}C resulting from the cycling of interstellar gas through stars of all masses over the lifetime of the Galaxy (provided ^{13}C is not purely a primary product; e.g., Prantzos et al. 1996). Although subject to a variety of uncertainties, this simple theory accounts well for the overall distance-$^{12}C/^{13}C$ and age-$^{12}C/^{13}C$ trends observed here and by others (e.g., Prantzos et al. 1996), as illustrated by the inset in Figure 2. Here the model predictions by Prantzos et al. (1996, their Fig. 3) are displayed against the $^{12}C/^{13}C$ ratios plotted as a function of distance to the Galactic center. The dashed line indicates the calculations where ^{13}C is assumed to be a mixed product of primary and secondary stellar processing, while the solid line depicts the results of a purely secondary ^{13}C contribution. Although there is sufficient scatter such that neither model can be ruled out, the results from the purely secondary calculations follow the observational gradient more closely.

An age–carbon isotope abundance effect is expected in the sense that the ISM $^{12}C/^{13}C$ decreases with time. The carbon isotope ratio was locked into the solar system 4.6 Gyr ago and represents the ISM abundance at that Galactic epoch in the region where the Sun formed. From equation (5), the average local present-day carbon isotope ratio is $^{12}C/^{13}C = 68 \pm 15$ at the Sun's distance, $D_{GC} = 7.9$ kpc (Fig. 2). This value is in agreement with very recent optical measurements of CH^+, which yield 78 ± 2 (Casassus et al. 2005). The hatched box (Fig. 2) represents the ranges in the (1) observed solar system $^{12}C/^{13}C$ abundance ratios and (2) calculated drift in galactocentric distance for the Sun over the past 4.6 Gyr (Wielen et al. 1996; Wielen & Wilson 1997). The abundance ratio range is set by the bulk values found for meteorites, comets, and interplanetary dust particles (IDPs), $^{12}C/^{13}C = 89 \pm 1$ (Clayton & Nittler 2004). The Sun's outward drift in galactocentric distance as a result of orbital diffusion over the past 4.6 Gyr can account for the Sun's overabundance in metals, $[Fe/H] = +0.17 \pm 0.04$, relative to the average metallicity of nearby F and G stars (Wielen et al. 1996). If the solar system were formed at 6.6 kpc, not 7.9 kpc, then the age–carbon isotope abundance difference is a 1 σ effect in the sense that the local ISM $^{12}C/^{13}C$ ratio has decreased by $\sim$30% over the past 4.6 Gyr (see Fig. 2), presumably due largely to ^{13}C enrichment of the ISM by AGB stars (Prantzos et al. 1996).

The dispersion in the $^{12}C/^{13}C$ abundance ratio for the sources observed in Figure 2 is roughly a factor of 2. At this level of significance we find no evidence for chemical fractionation effects. Since the Sun's metal abundance exceeds that of nearby stars, yet is about the same as metal abundances observed in local molecular clouds now forming stars in the Orion nebula, clearly an intrinsic dispersion in carbon isotope abundances exists, requiring more complex models of Galaxy formation and evolution to account for the intrinsic spread in Figure 2. Several possible explanations have been suggested to account for deviations from the basic simple GCE model (e.g., Olive & Schramm 1982; Pagel 1997; Binney & Merrifield 1998; Goswami & Vanhala 2000); among them are (1) cloud-to-cloud variations in molecular abundances due to initial chemical inhomogeneities (e.g., ejecta from local SNe or AGB stars) or differences in cloud chemistry and (2) Galactic dynamical effects such as cloud mergers, orbital diffusion, or radial gas streaming.

5. CONCLUSIONS

An independent measure of the $^{12}C/^{13}C$ isotope ratio has been measured across the Galaxy using the CN radical and its isotopomer. These ratios are in good agreement with past values derived from CO and H_2CO. These three molecules are formed by different chemical pathways; hence, fractionation effects in each species will occur via different mechanisms. The good agreement between $^{12}C/^{13}C$ ratios obtained from CO, CN, and H_2CO provides evidence against significant fractionation or isotope-selective photodissociation in molecular clouds. These measurements will help further establish the Galactic gradient and therefore enable more accurate models of GCE.

This research is supported by NASA through the NASA Astrobiology Institute under cooperative agreement CAN-02-OSS-02 issued through the Office of Space Science. The authors would like to thank Mark A. Smith, Department of Chemistry at the University of Arizona, for insight on how kinetic temperature affects the isotope ratio.

REFERENCES

Aoki, W., Inoue, S., Kawanomoto, S., Ryan, S. G., Smith, I. M., Suzuki, T. K., & Takada-Hidai, M. 2004, A&A, 428, 579
Apponi, A. J., Pesch, T. C., & Ziurys, L. M. 1999, ApJ, 519, L89
Binney, J., & Merrifield, M. 1998, Galactic Astronomy (Princeton: Princeton Univ. Press)
Blitz, L., Fich, M., & Stark, A. A. 1982, ApJS, 49, 183
Boothroyd, A. I., & Sackmann, I.-J. 1999, ApJ, 510, 232
Carral, P., & Welch, W. J. 1992, ApJ, 385, 244
Casassus, S., Stahl, O., & Wilson, T. L. 2005, A&A, 441, 181
Churchwell, E., Walmsley, C. M., & Wood, D. O. S. 1992, A&A, 253, 541
Clayton, D. D. 1983, Principles of Stellar Evolution and Nucleosynthesis (Chicago: Univ. Chicago Press)
———. 2003, Handbook of Isotopes in the Cosmos (Cambridge: Cambridge Univ. Press)
Clayton, D. D., & Nittler, L. R. 2004, ARA&A, 42, 39
Dickel, H. R., Dickel, J. R., & Wilson, W. J. 1981, ApJ, 250, L43
Gardner, F. F., & Whiteoak, J. B. 1979, MNRAS, 188, 331
Goldsmith, P. F., & Mao, X.-J. 1983, ApJ, 265, 791
Goswami, J. N., & Vanhala, H. A. T. 2000, in Protostars and Planets IV, ed. V. Mannings, A. P. Boss, & S. S. Russell (Tucson: Univ. Arizona Press), 963
Güsten, R., Henkel, C., & Batrla, W. 1985, A&A, 149, 195
Henkel, C., Güsten, R., & Gardner, F. F. 1985, A&A, 143, 148
Henkel, C., Walmsley, C. M., & Wilson, T. L. 1980, A&A, 82, 41
Henkel, C., Wilson, T. L., & Bieging, J. 1982, A&A, 109, 344
Henkel, C., Wilson, T. L., Walmsley, C. M., & Pauls, T. 1983, A&A, 127, 388
Herwig, F., & Austin, S. M. 2004, ApJ, 613, L73
Iben, I., Jr., & Renzini, A. 1983, ARA&A, 21, 271
———. 1984, Phys. Rep., 105, 329
Jaffe, D. T., Genzel, R., Harris, A. I., Lugten, J. B., Stacey, G. J., & Stutzki, J. 1989, ApJ, 344, 265
Keene, J., et al. 1998, ApJ, 494, L107
Kramer, C., Jakob, H., Mookerjea, B., Schneider, N., Brüll, M., & Stutzki, J. 2004, A&A, 424, 887
Langer, W. D. 1992, in IAU Symp. 150, Astrochemistry of Cosmic Phenomena, ed. P. D. Singh (Drodrecht: Kluwer), 193
Langer, W. D., Graedel, T. E., & Armentrout, P. B. 1984, ApJ, 277, 581
Langer, W. D., & Penzias, A. A. 1990, ApJ, 357, 477
———. 1993, ApJ, 408, 539
Le Teuff, Y. H., Millar, T. J., & Markwick, A. J. 2000, A&AS, 146, 157
Lis, D. C., & Goldsmith, P. F. 1991, ApJ, 369, 157
Mangum, J. G., Wootten, A., & Barsony, M. 1999, ApJ, 526, 845
Mangum, J. G., Wootten, A., & Mundy, L. G. 1991, ApJ, 378, 576
McNamara, D. H., Madsen, J. B., Barnes, J., & Ericksen, B. F. 2000, PASP, 112, 202
Olive, K., & Schramm, D. 1982, ApJ, 257, 276
Pagel, B. 1997, Nucleosynthesis and Chemical Evolution of Galaxies (Cambridge: Cambridge Univ. Press)
Penzias, A. A. 1980, Science, 208, 663
Prantzos, N., & Aubert, O. 1995, A&A, 302, 69
Prantzos, N., Aubert, O., & Audouze, J. 1996, A&A, 309, 760
Prasad, S. S., & Huntress, W. T., Jr. 1980a, ApJS, 43, 1
———. 1980b, ApJ, 239, 151
Savage, C., Apponi, A. J., Ziurys, L. M., & Wyckoff, S. 2002, ApJ, 578, 211
Timmes, F. X., Woosley, S. E., & Weaver, T. A. 1995, ApJS, 98, 617
van der Werf, P. P., Stutzki, J., Sternberg, A., & Krabbe, A. 1996, A&A, 313, 633
Watson, W. D., Anicich, V. G., & Huntress, W. T., Jr. 1976, ApJ, 205, L165
White, G. J., Phillips, J. P., Beckman, J. E., & Cronin, N. J. 1982, MNRAS, 199, 375
Wielen, R., Fuchs, B., & Dettbarn, C. 1996, A&A, 314, 438
Wielen, R., & Wilson, T. 1997, A&A, 326, 139
Wilson, T. L., & Rood, R. T. 1994, ARA&A, 32, 191
Wouterloot, J. G. A., & Brand, J. 1996, A&AS, 119, 439